INTERNATIONAL JOURNAL OF CIRCUITS, SYSTEMS AND SIGNAL PROCESSING
DOI: 10.46300/9106.2021.15.121 Volume 15, 2021

Simulation Optimization of Backrest Mechanism of Separable Bed Chair System

Meng Ning*, Zhi Wu, Lianjie Chen, Fan Zhang, Huitao Chen

Jiangsu Key Laboratory of Advanced Food Manufacturing Equipment & Technology, School of Mechanical Engineering, Jiangnan University, Wuxi 214122, Jiangsu, China

Received: March 20, 2021. Revised: August 11, 2021. Accepted: August 25, 2021. Published: August 26, 2021.

***Abstract*—Research and design an intelligent bed and chair integration system for assisting inconvenient mobility and aging population. The system consists of a removable detached wheelchair and a c-shaped bed with a fixed structure. The user can switch freely between the mobile wheelchair and the bed to meet the user's requirements of free movement and repositioning.Through the simulation software to analyze the movement characteristics of the bed backboard, the angle of the take-off and landing of the backboard and the sudden change of the take-off and abrupt angular velocity will cause the user to have dizziness and discomfort. In the case of determining the speed of the driving push rod, the relationship between mechanism parameters and installation parameters is the key to affect the lifting rate of the rear plate. Modeling and analysis of each mechanism is performed to determine the relationship between the mechanism parameters and the take-off and landing speed of the backplane. After optimizing the mechanism, the simulation is compared again to obtain the optimal solution. Finally, the optimal solution parameter is the final solution to improve the overall comfort of the nursing bed.**

***Index Terms*—Bed and chair integration system, abrupt angular velocity, dizziness, mechanism parameters, the overall comfort**

I. Introduction

IN recent years, the degree of aging of the population has increased, and it has also increased the risk of illness and disability among the elderly. In addition, the number of people suffering from physical injuries caused by frequent traffic accidents has also increased. It is difficult to walk and cannot take care of your status quo. One of the most laborious tasks in health care today is to move a bedridden person from bed to wheelchair [1]. This work is very labor-intensive, and the average person cannot continue for a long time without outside help. [2] Therefore, there is an urgent need for a device that can transfer easily and smoothly between the nursing bed and the wheelchair.

The devices to transform between the care-bed and the wheelchair have been developed by different groups in the last several years, e.g. the U-shape bed [3], the Multi-Functional Robotic Test-Bed [1,4], Hospital Bed with Auxiliary Functions [5,6], and an Automated Rehabilitation Bed [7]. These individual devices can be used to transfer the patients , but did not combine the functions of the bed and wheelchair.

A hybrid chair-bed system is designed and tested. The system can be used as both a wheelchair and a bed, and can automatically meet the needs of bedridden patients for transfer and repositioning. When used as a wheelchair, it helps the patient move freely. When used as a bed, the robotic system can help patients reorient themselves in a spacious space. It can help bedridden people live relatively independent lives; reduce the burden of families and medical staff.

During the test and testing of the prototype, some users, especially the older users felt some discomfort during the movement process of the prototype. After an investigation, we believe that the dramatic change of the speed and acceleration is the most important factor causing dizziness and discomfort in the movement of body by external forces. For the chair-bed system, the acceleration, deceleration and turning movement of the vehicle and the seat rotating movement relative to the vehicle may give users the feeling of motion sickness and dizziness; the movement of the bed plane, especially the lifting of the backplane may give users the feeling of constriction and dizziness. For the vehicle and seat, we can change the control parameters and reduce the maximum acceleration of the drive motor to improve comfort. But the drive of bed system is constant speed, unable to regulation by the control system. Therefore, we have proposed an optimizing design method to improve the using comfort through optimizing the mechanism acceleration during the kinematic processing. This method is applied to the improved design of the base plate mechanism of the chair bed system. Finally, the optimization results of the prototype are tested and compared.

II. Design concept

Figure 1 is a schematic diagram of the chair bed system, which consists of a reconfigurable mobile chair bed and a U-shaped bed. The chair-bed is consisted of a reconfigurable chair and a mobile vehicle. There is a mechanism fixed in the chair to help handle excretions. Between the chair and the

mobile vehicle, there equipped with a rotary axis, which built-in a motor drive mechanism and a locking mechanism, so that the chair can be rotating relative to the vehicle, as Figure 2 shows. Therefore, the chair bed can be converted between forward mode and lateral mode. The chair bed can be reconfigured as a flat bed or sofa with a recliner back and footrest. So the patient can be transferred by bed chair docking and bed chair separation.

Fig. 1. The docking process of the system

First, the patient drives the wheelchair close to the bed, then rotates the wheelchair to automatically guide the vehicle to the bed, and finally puts down the chair back and raises the footstool. When the bedridden wants to move away, first transform the chair bed into a chair type and automatically separate from the side of the bed. Then the chair is rotating and transformed from sideward mode to forward mode. To move the chair onto the bed, simply reverse the steps.

The mechanical structure is briefly introduced as Figure 2.

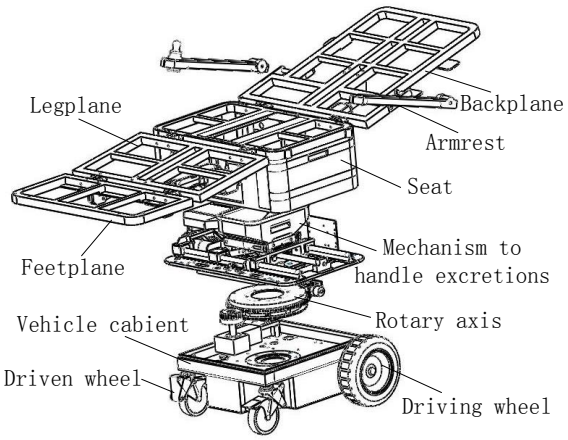

Fig. 2. The mechanical structure of the chair-bed

III. Mechanism Analysis

In order to meet the waterproof and low noise requirements of the electric medical-care equipment, the LINAK LA31 linear actuators are chosen to be the power sources of the mechanism. Taking into account space of the chair-bed system, backplane mechanism mainly consider two designs: a linear actuator is directly fixed between the backplane and the seat frame, that is called direct-drive mechanism; the linear actuator drive a roller pendulum to promote the backplane's movement, that is called indirect-drive mechanism.

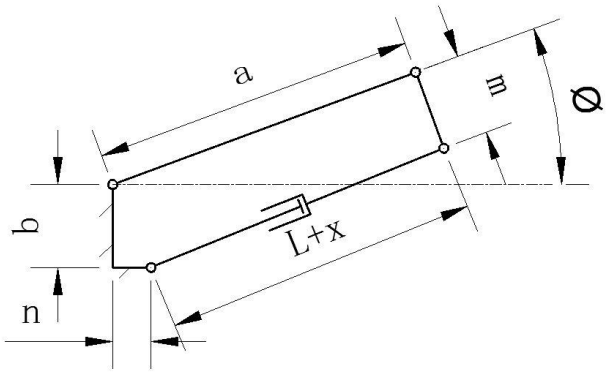

Fig. 3. The model of the direct-drive mechanism

The model of the direct-drive mechanism is shown as Figure 3. In the model, L is the original length of the linear drive, x is the stroke of the linear drive, a and m are the mounting parameters of the linear drive on the back plate, and b and n are the mounting parameters of the linear drive on the seat. Ø is the angle of the lifted backplane. From the knowledge of the geometry, we can easily get the following formula.

$$\begin{cases} \emptyset = A + B + C - \dfrac{\pi}{2} \\ tanA = \dfrac{n}{b} \\ 2\sqrt{a^2+m^2}\sqrt{b^2+n^2}cosA = a^2+b^2+m^2+n^2-(L+x)^2 \\ tanC = \dfrac{m}{a} \end{cases} \tag{1}$$

First-order partial derivatives of the above equations for x and Ø is as following

$$d\emptyset = \frac{\dfrac{(L+x)}{\sqrt{a^2+m^2}\sqrt{b^2+n^2}}}{\sqrt{1-\dfrac{\{a^2+b^2+m^2+n^2-(L+x)^2\}^2}{4(a^2+m^2)(b^2+n^2)}}}dx \tag{2}$$

Second-order partial derivative of the above equation for t is as following.

$$\begin{cases} \dfrac{d^2\emptyset}{dt^2} = \dfrac{\sqrt{\dfrac{D}{E}} - \dfrac{(L+x)^2\{a^2+b^2+m^2+n^2-(L+x)^2\}}{2E\sqrt{D\cdot E}}}{D}\dfrac{d^2x}{dt^2} \\ D = 1 - \dfrac{\{a^2+b^2+m^2+n^2-(L+x)^2\}^2}{4(a^2+m^2)(b^2+n^2)} \\ E = (a^2+m^2)(b^2+n^2) \end{cases} \tag{3}$$

From the above equations, we can obtain the relationship between the acceleration and various parameters.

The objective function is

$$Z = \min\left|\frac{d^2\emptyset}{dt^2}\right|, \left(\frac{d^2x}{dt^2} = M\right) \tag{4}$$

The constraint function is

$$\begin{cases} \emptyset = 0, (x = 0) \\ 72° \leq \emptyset \leq 83°, (x = max) \\ L = \max(x) + 188 \\ 70 \leq \max(x) \leq 250 \\ 50 \leq a \\ 50 \leq m \leq 300 \\ 50 \leq b \leq 300 \end{cases} \quad (5)$$

Arbitrary solving a set of feasible solutions β, and then as β a benchmark, separately change one parameter to observe the impact of the acceleration amplitude.

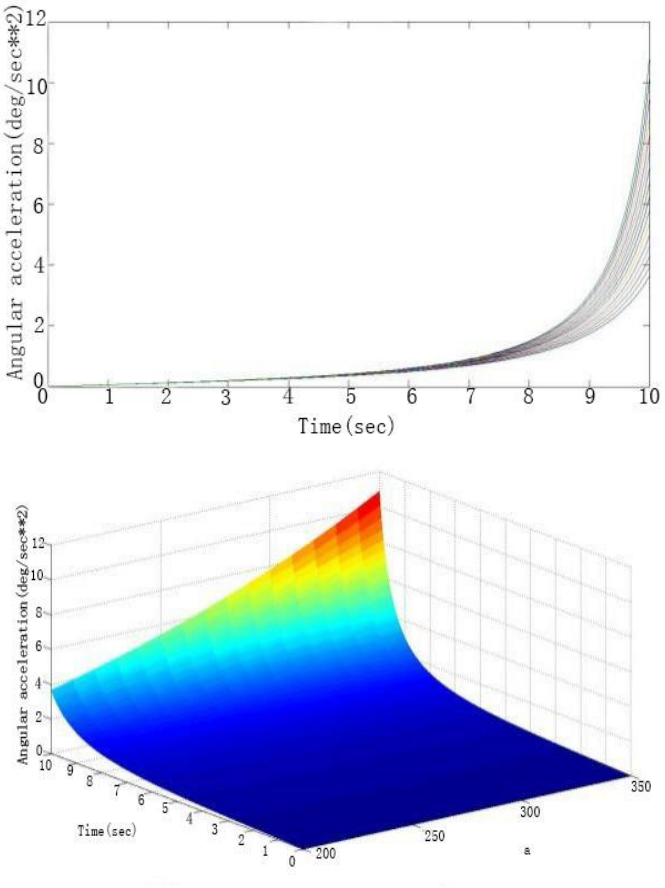

Fig. 4. Changes in angular acceleration with 'a'.

Figure 4 shows the changes of angular acceleration in the kinematic process from a = 200 to a = 350. It can be seen from the figure that during the movement of the direct drive mechanism, the angular acceleration of the back plate gradually increases from zero, and the trend of the initial change is slow and the final change is fast. The maximum angular acceleration of the rear plate occurs during the motion of the mechanism. The end of the process. As the parameter a increases, the maximum angular acceleration of the rear plate also increases, and the acceleration curve also becomes steeper.

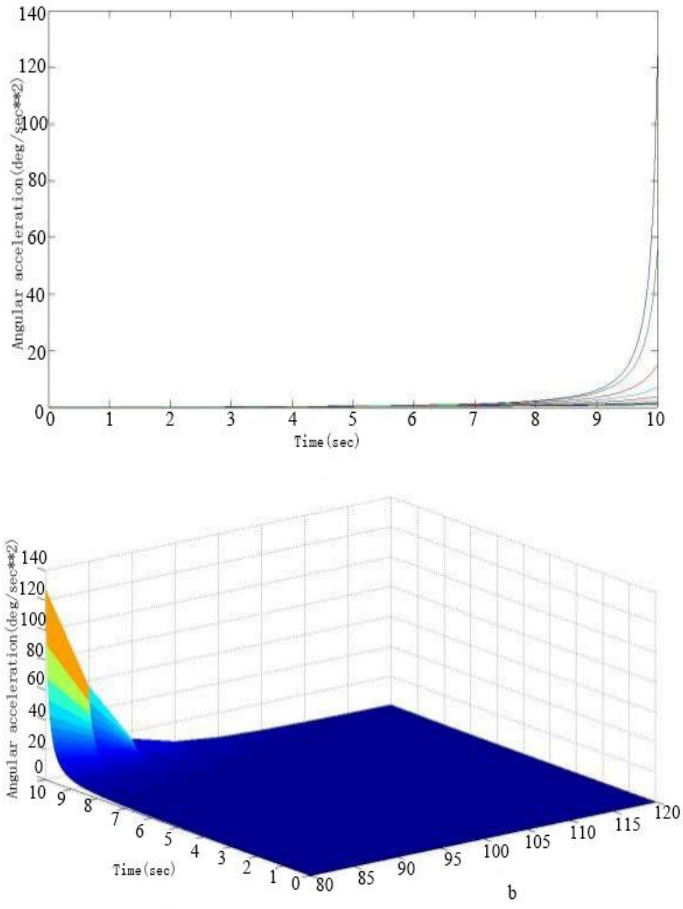

Fig. 5. Changes in angular acceleration with 'b'.

Figure 5 shows the changes of angular acceleration in the kinematic process from b = 80 to b = 120. It can be seen from the figure that when the parameter b≥95, the maximum angular acceleration of the backplane is almost independent of the change of the parameter b. When the parameter b is less than 90, the maximum angular acceleration of the backboard rises rapidly, and the acceleration curve also rapidly becomes Very steep.

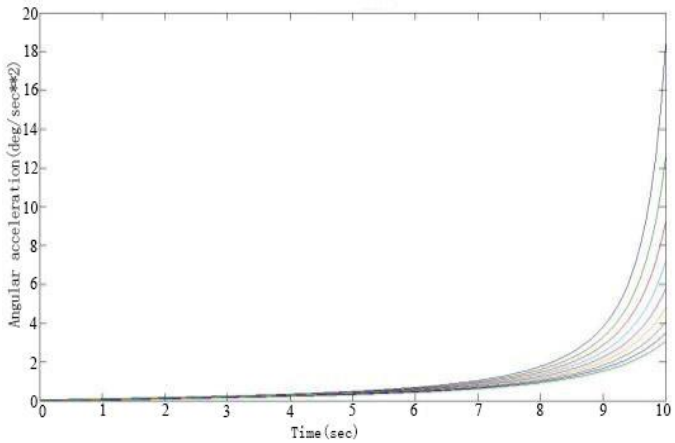

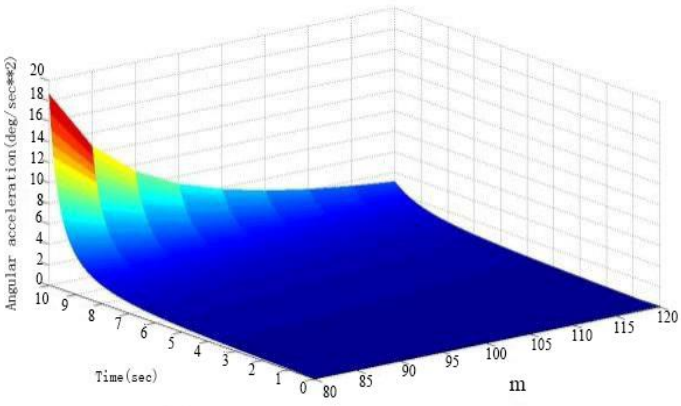

Fig. 6. Changes in angular acceleration with 'm'.

Figure 6 shows the changes of angular acceleration in the kinematic process from m = 80 to m = 120. It can be seen from the figure that as the parameter m gradually decreases, the maximum angular acceleration of the back plate also gradually increases, and the acceleration curve also becomes steeper.

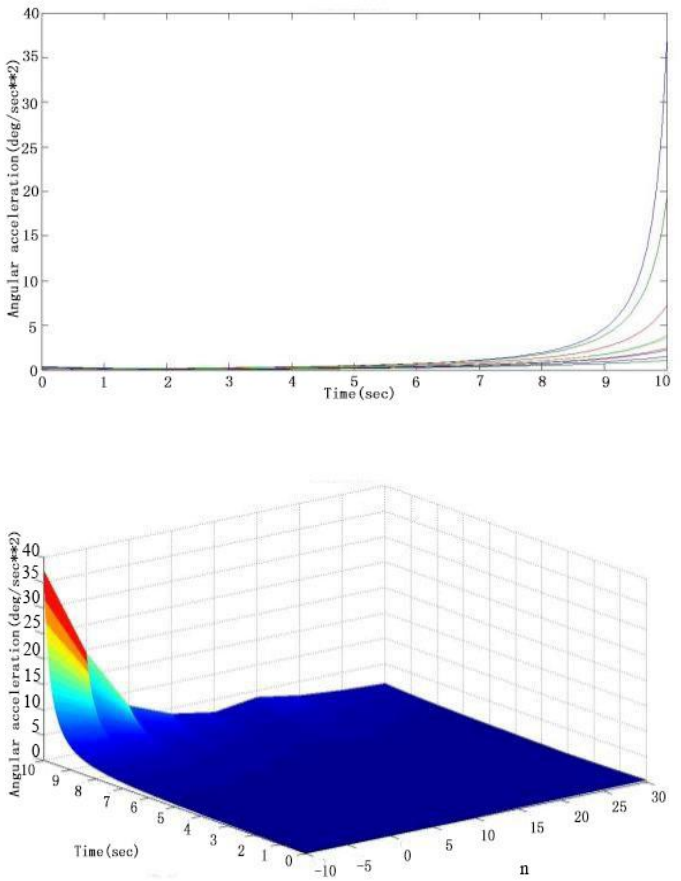

Fig. 7. Changes in angular acceleration with 'n'.

Figure 7 shows the changes of angular acceleration in the kinematic process from n = -10 to n = 30. It can be seen from the figure that when the parameter n≥0, the maximum angular acceleration of the backplane is almost independent of the change of n, but a high point appears at the point of n=10, which may be because the mechanism parameter is at this value. There is a singular point in the vicinity. When the parameter n<0, the maximum angular acceleration of the back plate increases sharply as the parameter n becomes smaller, and the angular acceleration curve of the back plate also becomes very steep.

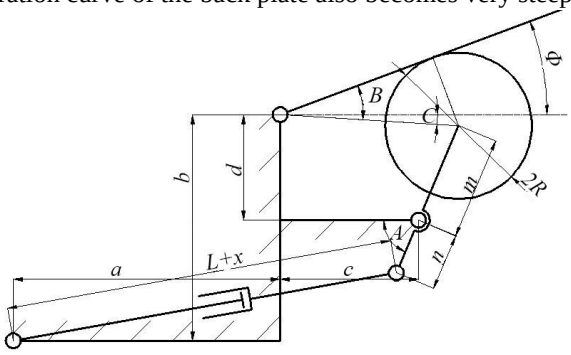

Fig. 8. The model of the indirect-drive mechanism

The model of the indirect-drive mechanism is shown as Figure 8. In the model, O is the hinge between the backplane and the seat, P is the hinge of the roller, L+x is the length of the liner actuator, a and b are the location of the hinge between the seat and the actuator relative to O, c and d are the location of the hinge between the pendulum and the seat relative to O, m+n is the length of the pendulum, R is the radius of the roller, ∅ is the angle of the lifted backplane. From the knowledge of the geometry, we can easily get the following formula:

$$\begin{cases} \emptyset = B - C \\ \mathrm{B} = \arcsin\dfrac{R}{OP} \\ OP = \sqrt{(\mathrm{c} + \mathrm{m}\cdot\cos\mathrm{A})^2 + (d - m\cdot sinA)^2} \\ C = arctan\dfrac{d - m\cdot sinA}{\mathrm{c} + \mathrm{m}\cdot\cos\mathrm{A}} \\ A = arctan\dfrac{b-d}{a+c} + arccos\dfrac{(a+c)^2 + (b-d)^2 + n^2 - (L+x)^2}{2n\cdot\sqrt{(a+c)^2 + (b-d)^2}} \end{cases} \quad (6)$$

From the above equations, we can obtain the relationship between the lifted angle ϕ and various parameters. Second-order partial derivative of the above equation for x and ϕ to t is too complex and hard to solve out, the relationship between $\frac{d^2\phi}{dt^2}$。 and $\frac{d^2x}{dt^2}$ can be directly solved by simulation methods.

Arbitrary solving a set of feasible solutions β, and then as B a benchmark, separately change one parameter to observe the impact of the acceleration amplitude.

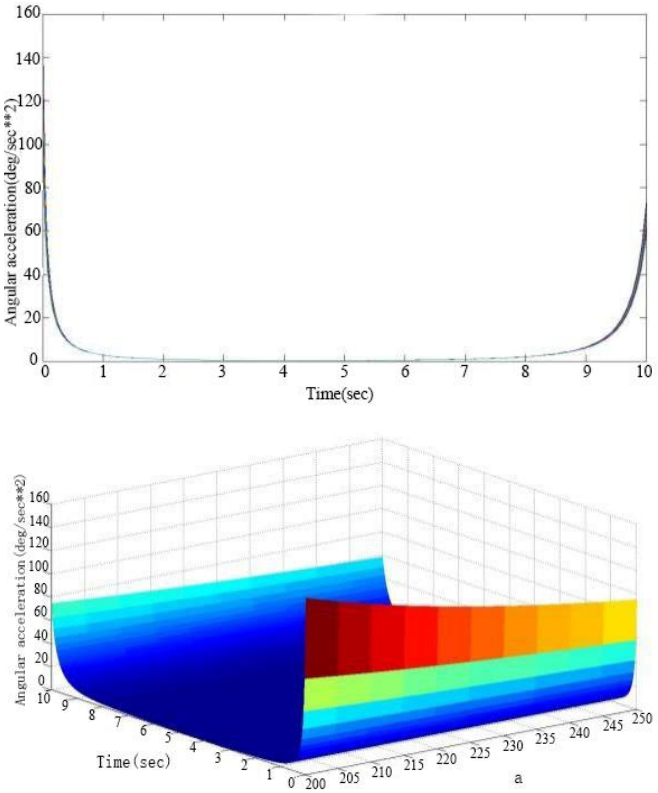

Fig. 9. Changes in angular acceleration with ‘a’.

Figure 9 shows the changes of angular acceleration in the kinematic process from a = 200 to a = 250. It can be seen from the figure that during the movement of the indirect drive mechanism, the angular acceleration of the back plate rapidly drops from the initial maximum value to a low value, and then remains stable until the final stage rapidly rises to the final maximum value. As the parameter a increases, the two maximum values of the angular acceleration of the backplane gradually decrease,and the absolute value of the initial maximum decreases faster than the final maximum.

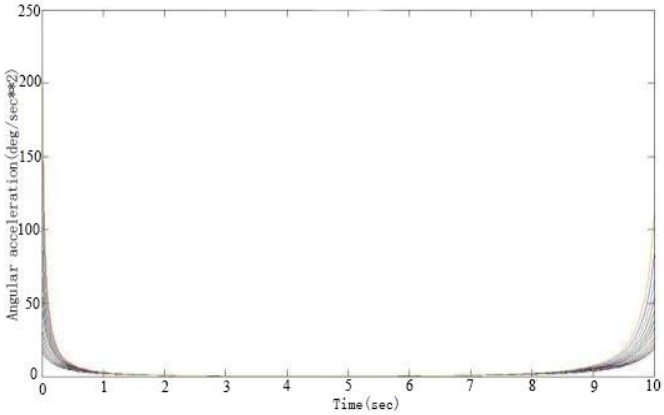

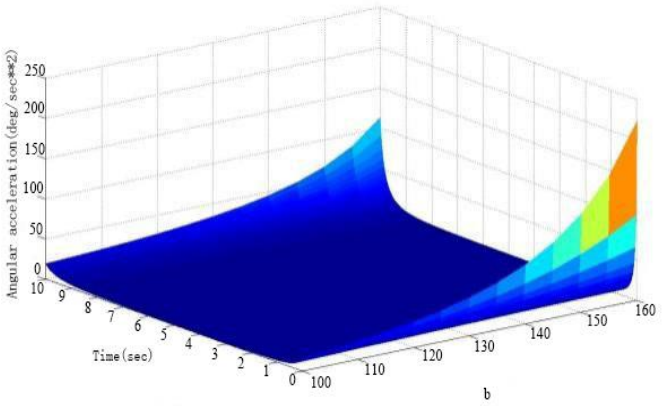

Fig. 10. Changes in angular acceleration with ‘b’

Figure 10 shows the changes of angular acceleration in the kinematic process from b = 100 to b = 160. As can be seen from the figure, with the increase of parameter b, the two maximum values of the angular acceleration of the backboard gradually increase, and the increasing speed becomes faster, and the absolute value and the increasing speed of the initial maximum value are always Higher than the final maximum.

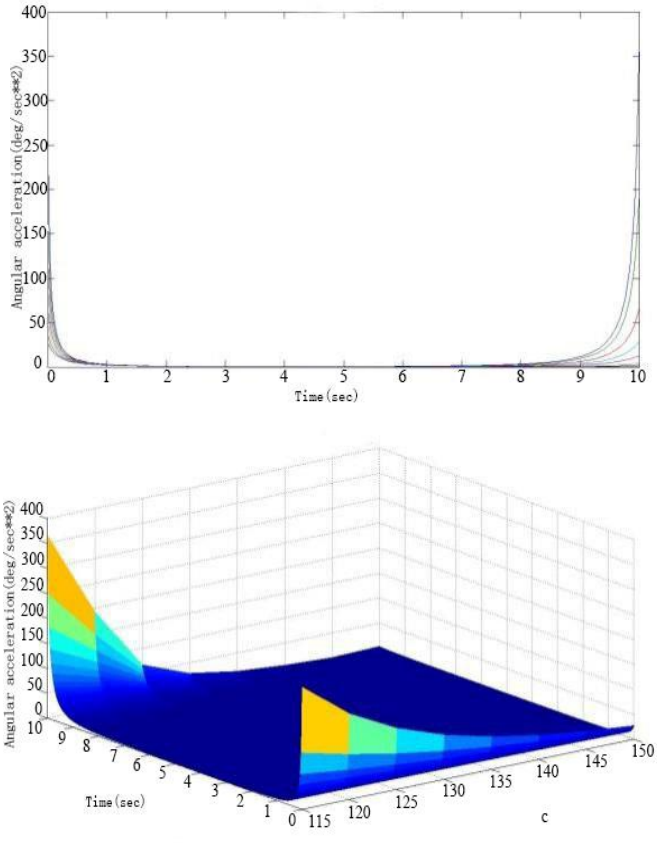

Fig. 11. Changes in angular acceleration with ‘c’

Figure 11 shows the changes of angular acceleration in the kinematic process from c = 115 to c = 150. As can be seen from the figure, with the increase of parameter c, the two maximum values of the angular acceleration of the backplane gradually

decrease. The initial maximum value is higher than the initial maximum value at the initial time, and the final pole increases with the increase of c.

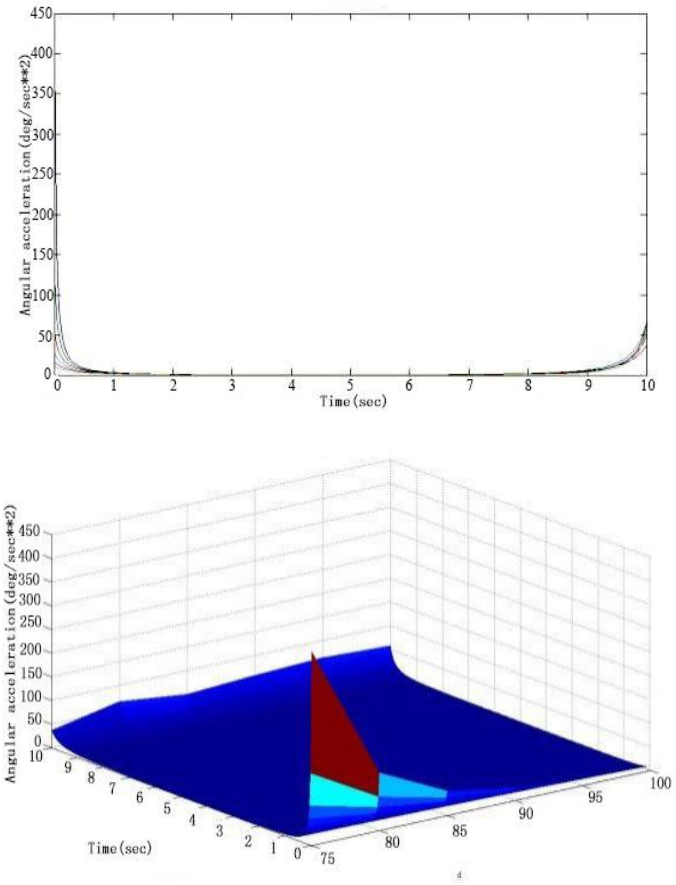

Fig. 12. Changes in angular acceleration with ‘d’

Figure 12 shows the changes of angular acceleration in the kinematic process from d = 75 to d = 100. As can be seen from the figure, with the increase of parameter d, the final maximum value of the angular acceleration of the backplane exhibits a small amplitude oscillation, while the initial maximum value is higher than the final maximum value at d=75, to d=90. The initial maximum has been reduced to the lowest value, so when d≥90, the final maximum is already higher than the initial maximum.

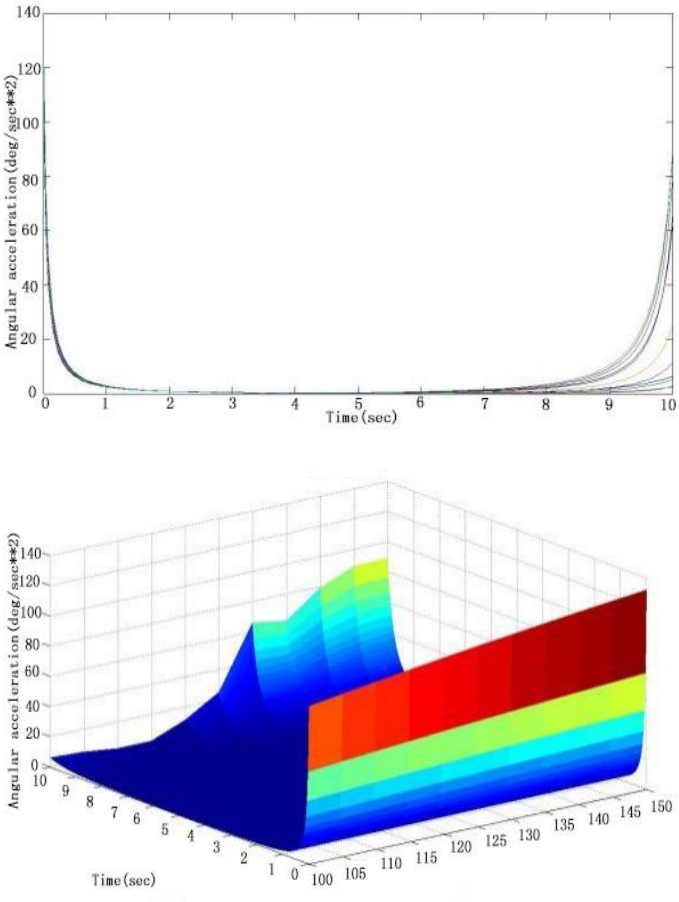

Fig. 13. Changes in angular acceleration with ‘m’

Figure 13 shows the changes of angular acceleration in the kinematic process from m = 100 to m = 150. As can be seen from the figure, with the increase of parameter m, the initial maximum value increases linearly, and the final maximum value initially shows a low value. When m=120, it increases rapidly, and then shifts to the oscillating rising state, but the initial pole Large values are always higher than the final maximum.

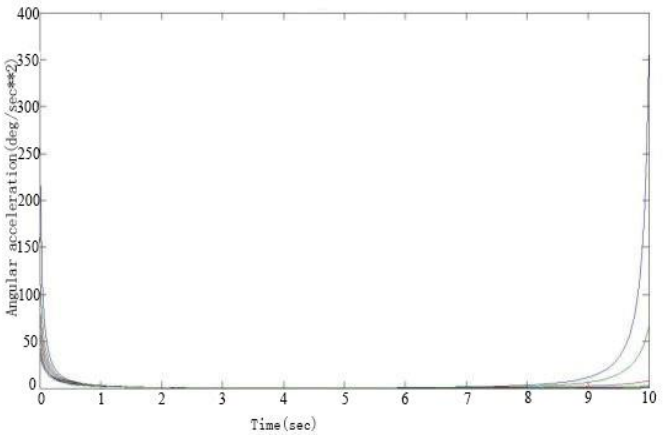

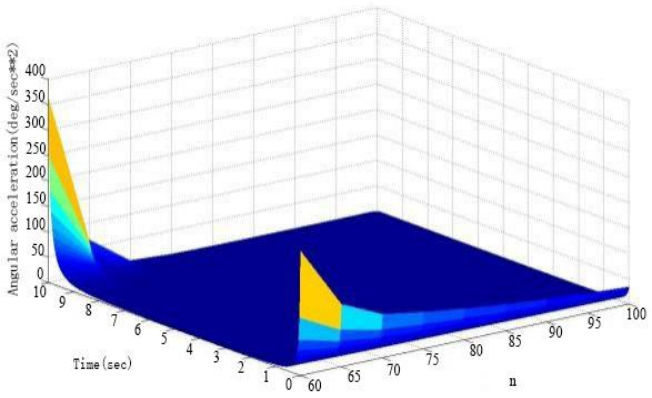

Fig. 14. Changes in angular acceleration with 'n'

Figure 14 shows the changes of angular acceleration in the kinematic process from n = 60 to n = 100. As can be seen from the figure, with the increase of parameter n, the two maximum values of the angular acceleration of the backplane gradually decrease. At the initial time, the final maximum value is higher than the initial maximum value, the initial maximum value shows a trend of decreasing first and then decreasing slowly, so when c≥70, the initial maximum value is already higher than the final maximum value.

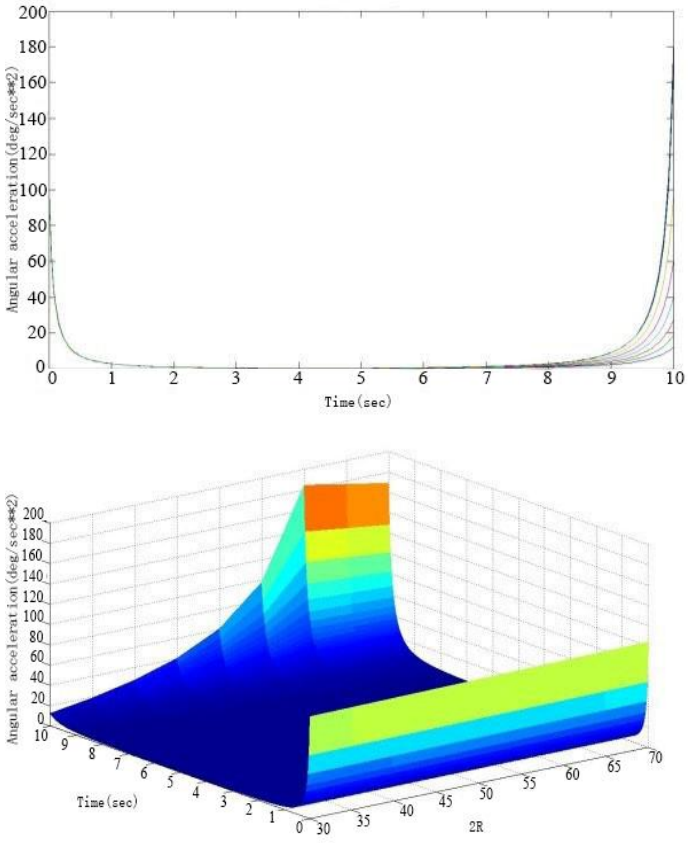

Fig. 15. Changes in angular acceleration with '2R'

Figure 15 shows the changes of angular acceleration in the kinematic process from 2R = 40 to 2R = 70. As can be seen from the figure, with the increase of parameter R, the initial maximum value of the angular acceleration of the backplane hardly changes, and the final maximum value gradually increases, and the increasing speed is faster and faster. After reaching the maximum to 2R=60, then slowly decreasing, the acceleration curve is also gradually steeper, and then slightly flattened. When 2R≥60, the final maximum value is already higher than the initial maximum value.

IV. Mechanism Design and Optimization

Through the simulation analysis of the direct drive mechanism above, the influence law and influence degree of the changes of the parameters of each mechanism on the acceleration of the backplane can be obtained. Combined with the boundary conditions of the backplane drive mechanism, a set of more optimized solutions γ can be solved by the graphical method, and compared with the reference solution β as follows:

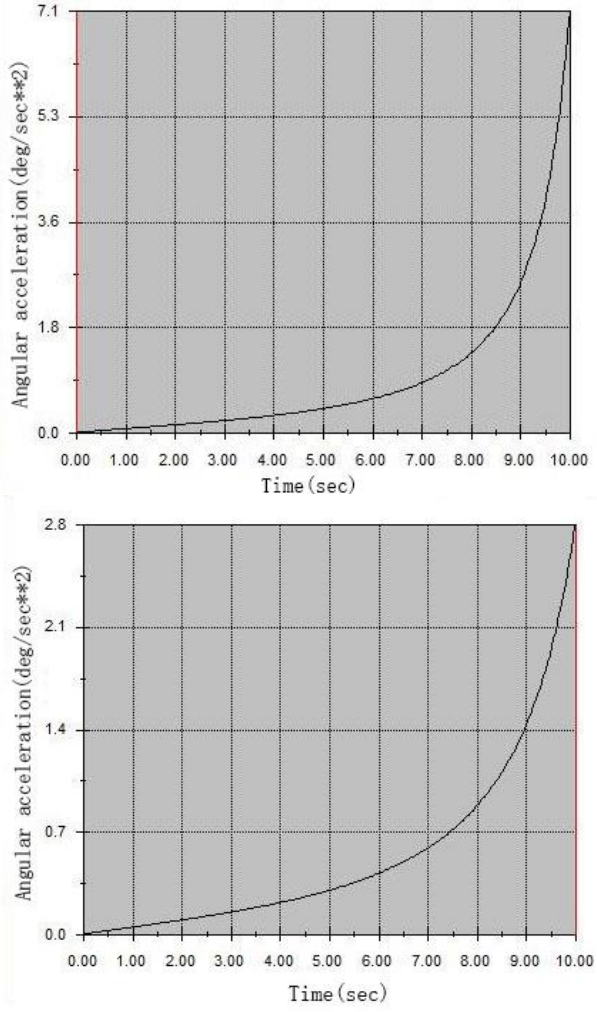

Fig. 16. The result of the direct-drive mechanism

As shown in Figure 16, the angular acceleration curve of the back plate is obtained by the reference solution β in the back-plate dynamics simulation. The mechanism parameters are a=290, m=95, n=95, b=0. The figure below shows the optimal solution γ. The angular acceleration curve has a mechanism

parameter of a=280, m=90, n=105, and b=0. It can be seen from the comparison that after optimization, the maximum angular acceleration of the rear plate is significantly reduced, and the angular acceleration curve is also smoother, and the mechanism optimization design has obvious effects.

Based on the above conclusion, considering the constraint function, the optimal solution γ can be solved through the graphical method, and contrasted with the benchmark solution β as below:

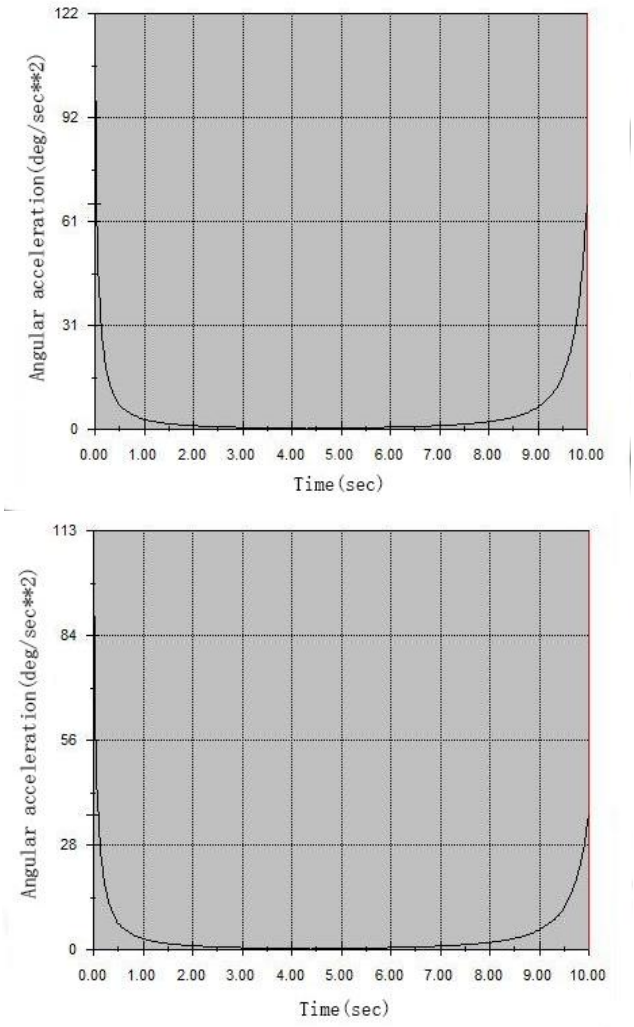

Fig. 17. The result of the direct-drive mechanism

As shown in Figure17, the angular acceleration curve of the back plate is obtained by the reference solution β in the backplane dynamics simulation. The mechanism parameters are a=220, b=150, c=125, d=80, m=130, n=65. R=25. The figure below shows the angular acceleration curve of the optimized solution γ. The mechanism parameters are a=225, b=145, c=135, d=80, m=140, n=65, R=27.5. It can be seen from the comparison that after optimization, the maximum angular acceleration of the rear plate is reduced, and the angular acceleration curve is also smoothed, but the optimization effect is not very obvious.

By comparing the direct drive mechanism with the indirect drive mechanism, it can be known that the maximum acceleration of the direct-drive mechanism is much smaller and the mechanism motion process is more smoothly.

V. Implementation and Experiment

Figure 18 shows an overall view of the chair-bed system developed by ITR. The system consists of a car, a chair bed and a U-shaped bed and is suitable for standard homes with minor modifications for elderly residents and bedridden patients. The left figure is the early version of the prototype, which is equipped with a direct-drive backplane mechanism as the benchmark solution. The right figure is the improved version. Comparing the early version, the problems are improved and the backplane mechanism is optimized.

Fig. 18. The overview of the chair-bed system

As shown in figure19, we invited 30 elderly users with good health to test the two prototypes independently. The tester's average age is 62 years, including 20 users over 55 years old. The different prototypes are numbered as A (early prototype), B (improved prototype). The testers were not aware of the number and distinction of the prototype. They only aware that this is a comfort evaluation experiment, and the comfort rating is required during the operation of the products through many movement process of backplane in order.

Fig. 19. The pictures during the test.

To avoid the deviation caused by the excessive attention to the single task, the experiment also required the comfort rating during the operation of the vehicle as an ancillary task. In the experiment, "comfort rating" is divided into five levels as Figure 20. The testers were divided into 3 groups, each including 10 testers, male and female are in equal. In the first

group, the odd testers will test the prototypes in the order of A-B independently, and the even testers are in the order of B-A. In the second group, the testers will only test the A prototype, and in the third group, the testers will only test the B prototype.

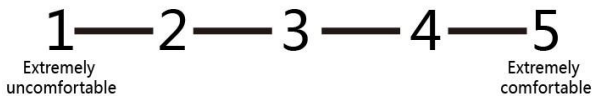

Fig. 20. The level of comfort rating

After the test, the comfort ratings of both functions are required, and only the result of the backplane function is analyzed. As shown in Table 1.

Table 1 . Result statistics

Tester	A	B	Tester	A	Tester	B
P1	4	4	P11	3	P21	4
P2	3	3	P12	4	P22	4
P3	3	4	P13	2	P23	3
P4	3	3	P14	3	P24	2
P5	4	3	P15	4	P25	3
P6	2	2	P16	4	P26	5
P7	4	4	P17	4	P27	4
P8	3	4	P18	3	P28	3
P9	3	3	P19	3	P29	3
P10	1	4	P20	2	P30	4
Average	3.1	3.45				
Male	3.4	3.5				
Female	2.8	3.4				

As shown in Figure21, through experiments, we found that more than half of the users cannot distinguish the difference between the prototypes in comfort. We believe that the main reason is that the movement of the backplane is very slow, the original maximum acceleration amplitude is not high, and acceleration changes are not dramatic.

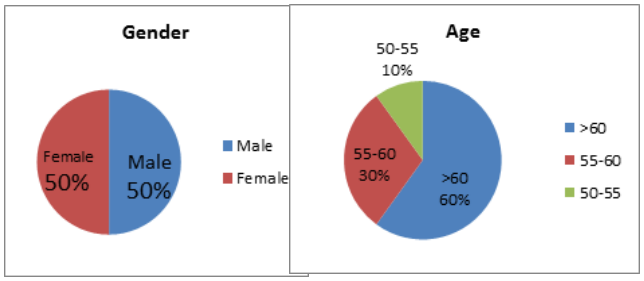

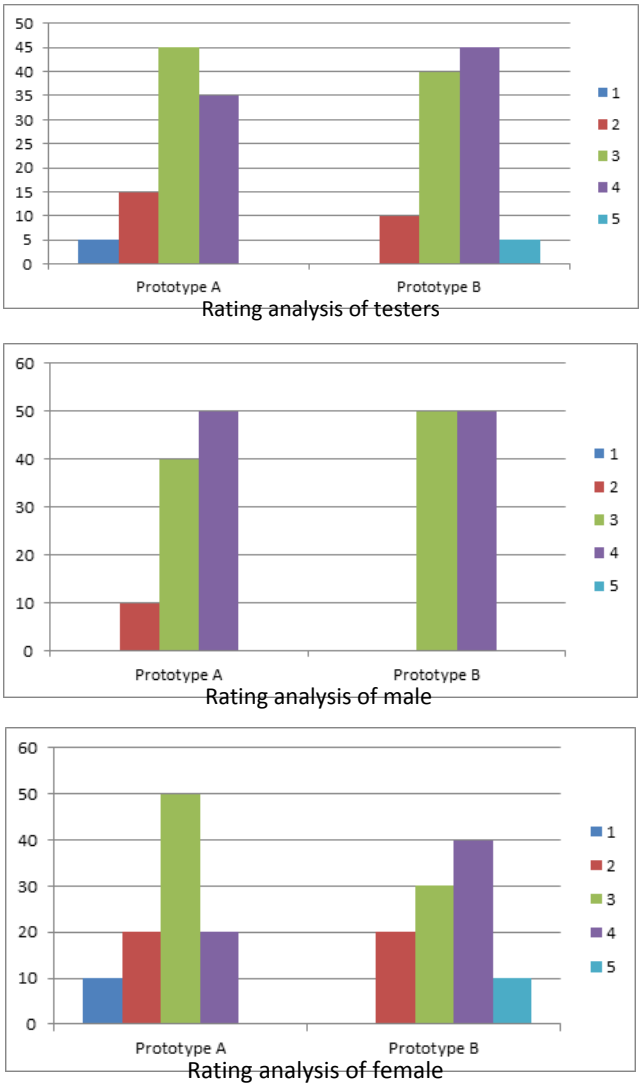

Fig. 21. Result analysis

Although after optimization, the kinematic parameters have been greatly improved, but the feeling of users is not very obvious. The vast majority of the rest users are considered that the improved prototype is more comfortable. It can be proved that the optimization played a certain effect on the feeling of users, and improve the using comfort of prototype significantly.

VI. Conclusion

In this paper, an optimal design method is proposed to improve the use comfort by optimizing the acceleration during kinematic processing, and the method is applied to the improved design of a robot chair-bed system. Through experiments and comparison tests, t can be proved that the optimization played a certain effect on the feeling of users. The prototype of the robotic chair-bed system has been successfully tested and implemented at the Sijiqing Nursing Home in Beijing. This method can be applied to other nursing bed systems and can significantly improve the comfort of use.

ACKNOWLEDGMENT

This work was supported by the Natural Science Foundation of Jiangsu Province, China (Grant No. BK20160185), Project supported by the National Science Foundation for Young Scientists of China (Grant No. 51705201), the Fundamental Research Funds for the Central Universities (Grant No. JUSRP11718), the Foundation of Jiangsu Key Laboratory of Advanced Food Manufacturing Equipment and Technology (Grant No. FM-2016-08), and the China Postdoctoral Science Foundation Funded Project (Project No.2018M630515).

REFERENCES

[1] X. Liang, X. Li, S. Jia and Y. Sun, "Wheelchair-bed docking control based on the combination of vision and ultrasound," 2017 Chinese Automation Congress (CAC), Jinan, 2017, pp. 4441-4446.

[2] Hu C M, Yeh C H. The synergy of QFD and TRIZ design practice — A case study for medical care bed[C]// International Conference on Modelling, Identification and Control. IEEE, 2011:523-531.

[3] W. Zou, A. Ye, T. Lu, Y. Ren, Z. Xu and K. Yuan, "Contour detection and localization of intelligent wheelchair for parking into and docking with U-shape bed," 2011 IEEE International Conference on Robotics and Biomimetics, Karon Beach, Phuket, 2011, pp. 378-383.

[4] F. Gómez-Rodríguez et al., "ED-Scorbot: A robotic test-bed framework for FPGA-based neuromorphic systems," 2016 6th IEEE International Conference on Biomedical Robotics and Biomechatronics (BioRob), Singapore, 2016, pp. 237-242.

[5] A. A. Bandala, L. K. G. Apelo, T. C. Dimalanta, J. V. V. Macatangay, J. E. S. Miciano and M. L. C. Sayo, "Development and design of automated hospital bed with incremental panels for bedsore prevention," TENCON 2014 - 2014 IEEE Region 10 Conference, Bangkok, 2014, pp. 1-6.

[6] C. Wang, A. V. Savkin, R. Clout and H. T. Nguyen, "An Intelligent Robotic Hospital Bed for Safe Transportation of Critical Neurosurgery Patients Along Crowded Hospital Corridors," in IEEE Transactions on Neural Systems and Rehabilitation Engineering, vol. 23, no. 5, pp. 744-754, Sept. 2015.

[7] B. Roy, A. Basmajan, H. H. Asada, "Repositioning of a Rigid Body with a Flexible Sheet and Its Application to an Automated Rehabilitation Bed", IEEE Transactions on Automation Science and Engineering, Vol.2 No.3, July 2005.